

Rapid Oxidation of SiC Using Microwave-Discharged O₂ Plasma at Low Temperatures (< 300°C)

Masataka SATOH*, Hisanori SHIMADA, Tomonori NAKAMURA and Sachiko YANAGIHARA

Research Center of Ion Beam Technology and College of Engineering, Hosei University, Koganei, Tokyo 184-8584, Japan

(Received September 10, 2001; accepted for publication January 5, 2002)

The rapid oxidation of 6H-SiC has been achieved using O₂ plasma, which is discharged by a microwave of 2.45 GHz at low temperatures below 300°C. X-ray photoelectron spectrometry (XPS) measurements reveal that O₂ plasma processing oxidizes SiC into the stoichiometric SiO₂ layer. The SiO₂ layer with a thickness of 22 nm is obtained after O₂ plasma processing for 10 min at a sample temperature of 200°C, which is 15 times faster than thermal oxidation in dry O₂ gas at 1150°C. There is a large amount of interface state at the SiO₂/SiC interface in an as-oxidized sample as well as in the case of the thermal oxidation. The formed SiO₂ layer shows a break down field strength of about 9.5 MV/cm, which is comparable to that of the thermal oxide layer. [DOI: 10.1143/JJAP.41.L233]

KEYWORDS: SiC, oxidation, O₂ plasma

Silicon carbide (SiC) is a prospective material for high temperature, high power and high frequency electron devices because of a wide band gap (about 3 eV for 6H-SiC), high breakdown field strength, and high saturation velocity of electrons.¹⁾ The stoichiometric SiO₂ layer produced by the thermal oxidation of SiC is utilized for the gate dielectric layer in a metal oxide semiconductor (MOS) field-effect transistor (FET) and the passivating and insulating layers in SiC electron devices,^{1–3)} which is a large advantage compared to other wide-band-gap semiconductors such as GaN and diamond. The electrical and structural properties of the thermally formed SiO₂ on SiC have been studied thoroughly.¹⁾ The thermal oxidation of SiC is carried out at temperatures above 1150°C and the growth rate of the SiO₂ layer on Si face of (0001)-oriented SiC is very slow compared to that of Si. The slow growth rate of SiO₂ on SiC by thermal oxidation is a disadvantage in the fabrication of a thick insulating-layer between the devices on SiC.

On the other hand, in the Si technology, the O₂ plasma oxidation of Si has been studied thoroughly.^{4–6)} In the oxidation of Si using the microwave-discharged O₂ plasma, the oxidation rate is larger than in the case of the thermal oxidation at 1000°C. Although the mechanism of plasma oxidation of Si has not been yet understood, it is expected that O₂ plasma oxidation is useful for the reduction of the oxidation temperature and the enhancement of the oxidation rate.

Lucovsky *et al.*⁷⁾ have reported that SiC can be oxidized by remote plasma-assisted oxidation, in which the oxidation rate is much smaller than that of thermal oxidation. However, it is well known that the number of radical species in the plasma strongly depends on the pressure, power of the microwave, and structure of the plasma equipment.⁵⁾ Since low-pressure plasma would contain a large amount of ionized and excited neutral O radicals, the growth rate of SiO₂ on SiC could be improved using low-pressure O₂ plasma.

In the present letter, we report the O₂ plasma oxidation of 6H-SiC. The O₂ plasma processing of 6H-SiC at a pressure of 100 mTorr shows a rapid oxidation rate at temperatures below 300°C.

The samples used in this study were n-type 6H-SiC epitax-

ial layers grown on the (0001)-oriented n-type 6H-SiC substrates, which were provided by Cree Research. The net doping concentration of an epitaxial layer was about $1 \times 10^{16}/\text{cm}^3$. After a standard cleaning of the sample, O₂ plasma oxidation was carried out at sample temperatures below 300°C using microwave plasma equipment with a 500 W magnetron tube. The sample was located at a distance of 15 mm from the bottom of the reaction tube. The Ar and O₂ flow rates were 5.6 and 0.4 sccm, respectively, and the pressure of gas in the chamber was fixed at 100 mTorr during the plasma processing. Ar gas was introduced into the chamber to enhance the excitation of O radicals in the discharged plasma.⁵⁾

The composition of the formed oxide layer was evaluated using X-ray photoelectron spectrometry (XPS) with a Mg X-ray source. In the XPS measurements, a neutralizer was used to suppress the charge-up of the sample. The thickness of the oxide layer was evaluated by either ellipsometry with a He-Ne laser or a Tencor Alpha Step 500 profilometer. The electrical properties of the formed oxide layer were evaluated by means of high-frequency capacitance–voltage (*C*–*V*) and current–voltage (*I*–*V*) measurements at room temperature. In these measurements, the back ohmic contact at the back surface of the sample was formed by annealing the deposited NiSi₂ at 900°C for 10 min in Ar + H₂ ambient,⁸⁾ and subsequently, an Al gate electrode with a diameter of 0.3 mm was deposited on the SiO₂ surface. *C*–*V* measurement was carried out at a frequency of 1 MHz.

Figure 1 shows XPS spectra obtained from the oxide layer on 6H-SiC formed using O₂ plasma. The binding energies of Si 2p (103 eV) and O 1s (532 eV) electrons in the O₂-plasma-oxidized layer are identical to those of the thermally oxidized SiO₂ layer of SiC. It is indicated that SiC can be oxidized into SiO₂ using the O₂ plasma as well as in the case of the thermal oxidation of SiC. Note that there are no pronounced signals from C atoms in the SiO₂ layer. The signals of C 1s at the top-most surface may be produced from the surface contamination during the transportation of the sample in atmosphere. Since the diffusivity of C atom in the SiO₂ layer is negligibly small at 200°C,⁹⁾ it is suggested that O₂ plasma processing promotes the diffusion of C atoms from the surface of the SiO₂ layer.

At a depth corresponding to the SiO₂/SiC interface (indicated by arrows in Fig. 1), there is a transient layer from SiO₂

*E-mail address: mah@ionbeam.hosei.ac.jp. Tentative address: Electrical and Computer Engineering, Purdue University, 1285 Electrical Engineering Building, West Lafayette, IN 47907-1285, U.S.A.

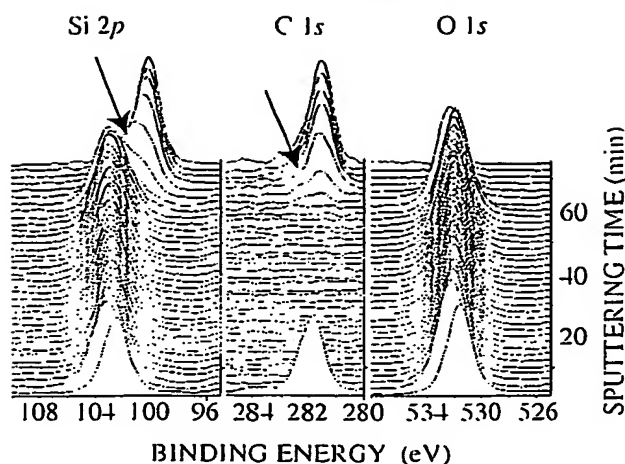


Fig. 1. XPS spectra taken from the O_2 plasma-oxidized SiO_2 layer on 6H-SiC. Arrows indicate a depth corresponding to the interface between SiO_2 and SiC.

to SiC in XPS spectra for Si 2p and C 1s, which is similar to that of the thermal oxide layer.¹⁰⁾ In the case of the plasma oxidation of Si, the oxidation of Si occurs at the SiO_2 /Si interface by the migration of active oxygen atoms or ions toward the interface accompanied by oxygen exchange in the grown SiO_2 layer.¹¹⁾ In the plasma oxidation of SiC, since the composition of the oxide layer is identical to that of SiO_2 , it is suggested that the oxidation of SiC occurs at the SiO_2 /SiC interface, which results in the formation of the transient layer at the interface as in the case of the thermal oxidation of SiC.

Figure 2 shows the oxide thickness as a function of the oxidation time. The oxidation rate for dry thermal oxidation at 1150°C for Si-face of 6H-SiC is also shown. For the Si-faced sample, the SiO_2 layer with a thickness of 74 nm was obtained after plasma oxidation for 20 min, while that for the thermal oxidation was evaluated to be 2 nm for Si-face of 6H-SiC. Furthermore, the oxide thickness for C-face is greater than that for Si-face. The oxidation rate of C-face is higher than that of Si-face in O_2 plasma oxidation, which is similar to the case of the thermal oxidation of (0001)-oriented SiC. The oxidation time dependences of the oxide thickness for Si- and C-faces show slopes of 1.5 and 0.75 to the oxidation time of 30 min, and 0.4 and 0.2 beyond the oxidation time of 30 min, respectively, while the slope of thermal oxidation is estimated to be 1.0, which is related to the reaction-controlled oxidation at the SiO_2 /SiC interface. For the plasma oxidation of the C-faced SiC sample, the obtained slopes are in good agreement with those in the case of Si. The initial growth with a slope of 0.72 is related to both Si-SiO₂ interface reaction-controlled and diffusion-controlled oxidation in the SiO_2 layer, while the growth with a slope of 0.2 is correlated to the Cabrera-Mott model.⁶⁾ The plasma oxidation of Si-faced SiC shows 2-fold slopes larger than that of C-faced SiC all for oxidation times. Unknown phenomena may be involved in the plasma oxidation of Si-faced SiC. The activation energy of the plasma oxidation of 6H-SiC was estimated to be approximately 0.04 eV for both Si- and C-face in the temperature range from 100 to 300°C . The low activation energy indicates that the plasma oxidation is predominantly activated by O_2 plasma processing of SiC. Furthermore, the spectrometry of the O_2 plasma reveals that there is a large amount of

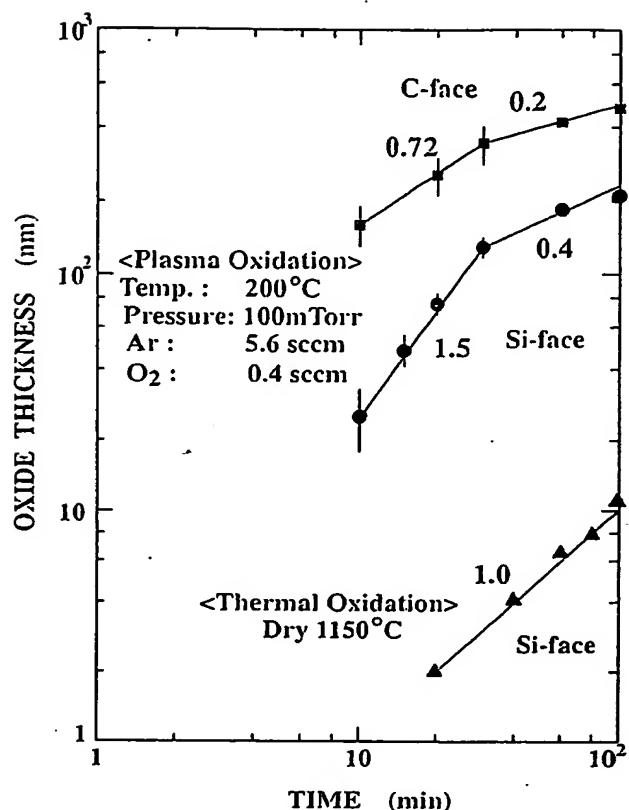
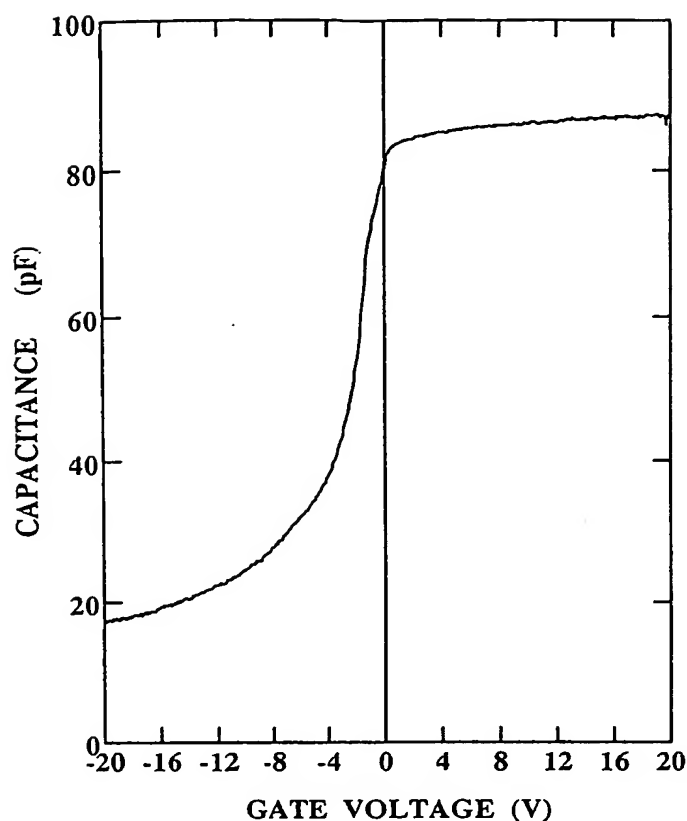


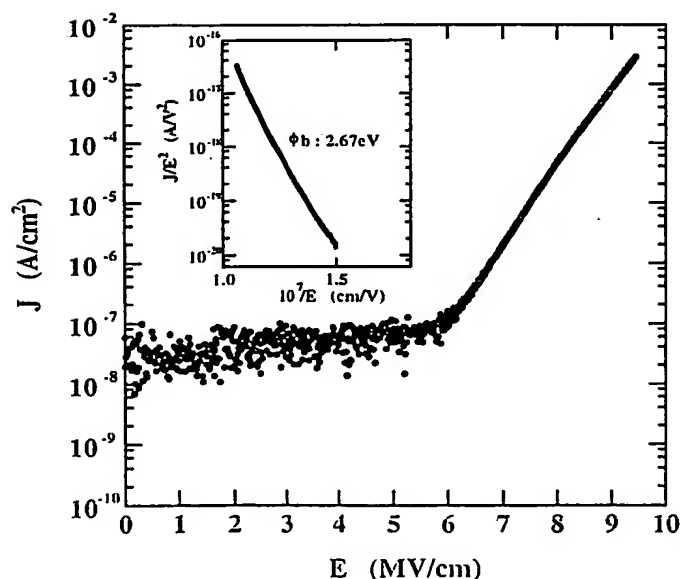
Fig. 2. Oxidation time dependence of oxide thickness for the O_2 plasma oxidation of n-type 6H-SiC. The oxide thickness for dry O_2 thermal oxidation is also shown.

ionized O radicals in the discharged plasma at a pressure of 100 mTorr, while the O_2 plasma at a pressure above 150 mTorr consists of neutral O_2 radicals (data not shown). In the case of the O_2 plasma processing involving no ionized O radicals, the oxidation rate is very slow. It is suggested that the ionized O radicals are involved in the plasma oxidation mechanism.

Figures 3(a) and 3(b) show the results of C-V and I-V measurements for the as-oxidized sample with an oxide thickness of 40 nm, respectively. In the C-V measurement, the C-V curve suggests the existence of a large amount of interface state at the SiO_2 /SiC interface which has also been observed in the thermally oxidized SiC without any post-oxidation annealing. The large amount of the interface state is related to the transient layer at the interface as observed in the XPS spectra (see Fig. 1). The average density of the interface state was estimated to be in the order of $10^{13}/\text{eV}\cdot\text{cm}^2$ by comparing the obtained C-V curve with the theoretical curve. It has been reported that the density of the interface trap can be reduced by the post-oxidation annealing in either wet O_2 ambient¹²⁾ or H_2 gas ambient.¹³⁾ To examine the effect of post-oxidation annealing, the plasma-grown SiO_2 /SiC sample was annealed at 950°C in Ar + H_2 ambient up to 1 h. However, it was observed that the post-oxidation annealing does not decrease the density of the interface trap. In I-V characterization, the breakdown field strength was estimated to be 9.5 MV/cm, which is comparable to that of the thermally oxidized films (9.7 MV/cm, not shown). In the electric field strength ranging from 6.0 to 9.5 MV/cm, the Fowler-Nordheim current¹⁴⁾ can be observed. The inset in Fig. 3(b)



(a)



(b)

Fig. 3. (a) C - V and (b) I - V characteristics of the O_2 plasma oxidized SiO_2 layer on n -type 6H-SiC epitaxial films. The oxide thickness is about 40 nm. The inset shows the Fowler-Nordheim plot for the obtained I - V characteristics.

shows the Fowler-Nordheim plot for the O_2 -plasma-oxidized SiO_2 layer on n -type SiC. Using the effective electron mass of 0.42 m , where m is the mass of a free electron, the barrier height from the Fermi level to the bottom of the conduction band of SiO_2 was estimated to be 2.67 eV, which is similar to that of the thermally oxidized SiO_2 layer on n -type SiC (2.69 eV).

In summary, we reported the rapid oxidation of n -type 6H-SiC(0001) at temperatures below 300°C using a microwave-discharged O_2 plasma. The O_2 plasma oxidation rate was 15 times faster than that of the thermal oxidation at 1150°C. The O_2 -plasma-oxidized layer on SiC was stoichiometric SiO_2 except for the interface. The C - V and I - V measurements revealed that the electrical properties of the plasma-oxidized SiO_2 layer are comparable to those of the thermally oxidized SiO_2 layer on SiC. We can conclude that O_2 plasma oxidation process is useful for the reduction of the process temperature and the enhancement of the oxidation rate of SiC. The mechanism of O_2 plasma oxidation and the effect of post-oxidation annealing on the electrical properties will be published elsewhere.

Authors wish to express thanks to Professor Nakamura for the use of the plasma equipment and the micro probe station.

- 1) *Silicon Carbide*, ed. G. L. Harris (INSPEC, London, 1995) EMS Databooks Series No. 13.
- 2) J. A. Powell, J. B. Petit, J. H. Edgar, I. G. Jenkins, J. G. Matus, W. J. Choyke, L. Clemen, M. Yoganathan, J. W. Yang and P. Pirouz: *Appl. Phys. Lett.* **59** (1991) 183.
- 3) J. N. Shenoy, J. A. Cooper, Jr. and M. R. Melloch: *IEEE Electron Device Lett.* **18** (1997) 93.
- 4) K. Eljabaly and A. Reisman: *J. Electrochem. Soc.* **138** (1991) 1071.
- 5) S. Dzioba, G. Este and H. M. Naguib: *J. Electrochem. Soc.* **129** (1982) 2537.
- 6) Y. Kawai, N. Konishi, J. Watanabe and T. Ohmi: *Appl. Phys. Lett.* **64** (1994) 2223.
- 7) G. Lucovsky and H. Niimi: *Mater. Sci. Forum* **264-268** (1998) 1021.
- 8) T. Nakamura, H. Shimada and M. Satoh: *Mater. Sci. Forum* **338-342** (2000) 985.
- 9) I. Mizushima, E. Kamiya, N. Arai, M. Sonoda, M. Yoshiki, S. Takagi, M. Wakamiya, S. Kambayashi, Y. Mikata, S. Mori and M. Kashiwagi: *Jpn. J. Appl. Phys.* **36** (1997) 1465.
- 10) C. Radtke, I. J. R. Baumvol, J. Morais and F. C. Stedile: *Appl. Phys. Lett.* **78** (2001) 3601.
- 11) S. Kimura, E. Murakami, T. Warabisako, E. Mitani and H. Sunami: *J. Appl. Phys.* **63** (1988) 4655.
- 12) G. G. Jernigan, R. E. Stahlbush and N. S. Saks: *Appl. Phys. Lett.* **77** (2000) 1437.
- 13) K. Fukuda, S. Suzuki, T. Tanaka and K. Arai: *Appl. Phys. Lett.* **76** (2000) 1585.
- 14) P. Friedrichs, E. P. Burte and R. Schorner: *Appl. Phys. Lett.* **65** (1994) 1665.

Plasma-assisted formation of low defect density SiC–SiO₂ interfaces

A. Götz

Institut für Halbleitertechnik, RWTH-Aachen, Aachen D-52074, Germany

G. Lucovsky,^{a)} K. Koh, D. Wolfe, and H. Niimi

Departments of Physics, Materials Science and Engineering and Electrical and Computer Engineering, and Chemistry, North Carolina State University, Raleigh, North Carolina 27695-8202

H. Kurz

Institut für Halbleitertechnik, RWTH-Aachen, Aachen D-52074, Germany

(Received 24 February 1997; accepted 22 April 1997)

The initial stages of SiC–SiO₂ interface formation by low temperature (300 °C) remote plasma assisted oxidation (RPAO) on flat and vicinal 6H SiC(0001) wafers with Si faces have been studied by on-line Auger electron spectroscopy (AES). Changes in AES spectral features associated with Si–C and Si–O bonds are readily evident as oxidation progresses; however, there are no detectable AES features that can be attributed to C–O bonds. Initial oxidation rates as determined from AES data are greater for vicinal wafers than for flat wafers paralleling results for RPAO oxidation of Si. Devices fabricated on vicinal SiC wafers require a 1150 °C anneal in an H₂ containing ambient to reduce defect densities from the 10¹³ to 10¹¹ cm^{–2} range, consistent with termination of C atom step edge dangling bonds by H atoms. Devices prepared by thermal oxidation also require a 1150 °C anneal in H₂ even though silicon oxycarbide regions with C–O bonds are formed in a transition region at the SiC–SiO₂ interfaces. © 1997 American Vacuum Society. [S0734-211X(97)07304-6]

I. INTRODUCTION

There is considerable interest in SiC for high temperature device applications, including power transistors. To fabricate these devices, it will be necessary to gain an increased understanding of the chemical bonding at the SiC–SiO₂ interface, and in particular to develop processing that minimize interfacial defects and transition regions, and maximize device reliability as manifested in reductions in the rate of interfacial and bulk defect generation during operation. It has been established that the oxide that forms on SiC during high temperature oxidation in O₂ ambients is SiO₂, and that this oxidation process can yield SiC–SiO₂ interfaces and gate dielectrics with sufficiently low defect densities for field effect transistor (FET) operation.¹ However, channel mobilities at room temperature (in depletion mode FETs) are significantly lower than expected from bulk SiC properties and much research has been focused on explaining these differences and improving channel mobilities.² Since SiO₂ is the dominant solid state oxidation product, oxidation products involving carbon atoms must include gaseous molecules such as CO; as oxide growth progresses these must be transported from the buried growth interface through the oxide and out of the film. However, this does not preclude the formation of additional interfacial carbon atom bonding arrangements such as Si–C and C–O as have been reported in silicon oxycarbide transition regions.³ The molar volume mismatch between SiC and SiO₂ is greater than the corresponding mismatch between Si and SiO₂, so that intrinsic levels of strain at SiC–SiO₂ interfaces are anticipated to be at least as high as the values of approximately 5 × 10⁹ dynes/cm² reported in Si–SiO₂.⁴ This article deals

with an alternative low temperature method for semiconductor-dielectric interface formation that has been successfully applied to crystalline Si device technology.^{5,6} As applied to Si, this approach provides independent control of Si–SiO₂ interface formation and dielectric film growth. The Si–SiO₂ interface and a superficially thin oxide layer (~0.5 nm) are formed by a low temperature (300 °C) remote plasma-assisted oxidation (RPAO) process, and the remainder of the oxide layer is deposited by a low temperature (300 °C) remote plasma enhanced chemical vapor deposition (RPECVD) process. Device quality interfaces are obtained by subjecting the plasma processed Si–SiO₂ heterostructure to a post-deposition rapid thermal anneal (RTA), e.g., for 30 s at 900 °C. The 900 °C anneal promotes both chemical and structural interface relaxations, including a minimization of interfacial sub-oxide bonding arrangements in transition regions between the Si crystal and the stoichiometric bulk oxide.⁷ A similar plasma-assisted process has recently been applied to SiC, and has yielded SiC–SiO₂ interfaces with defect state densities comparable to what has been achieved on SiC by conventional high temperature thermal oxidation.⁸ The potential advantages of this two step approach to SiC–SiO₂ interface formation are: (i) it reduces the requirement for transporting gaseous reaction products such as CO molecules away from the interface as the oxide grows; and (ii) it can also reduce strain induced interface defect generation, since only a small fraction of the total oxide layer thickness is generated by consumption of the SiC substrate. The focal point of this article is a study of SiC–SiO₂ interface formation by RPAO using on-line Auger electron spectroscopy (AES) to monitor interface bonding chemistry and the initial oxide growth rate.

Before discussing the SiC AES measurements, it is useful

^{a)}Electronic mail: gerry_lucovsky@ncsu.edu

to summarize the results of device studies on vicinal Si and SiC wafers using the plasma-assisted processing steps identified above. Studies by Bjorkman *et al.*⁹ demonstrated that densities of mid-gap defect states (D_{it}) as low as $1 \times 10^{10} \text{ cm}^{-2} \text{ eV}^{-1}$ could be obtained on Si(111) surfaces by using conventional thermal oxidation, metal electrodes and 400 °C post metal anneals in an H₂ containing ambient. Previous studies had always shown higher values for Si(111) as compared to the Si(100) surfaces used in the integrated circuit wafers (see Reference 9). Studies performed by Yasuda *et al.* on *p*-type Si(111) vicinal up to 5° in the 112 direction showed that the density of mid-gap states (D_{it}) increased by relatively small amounts from $\sim 1 \times 10^{10} \text{ cm}^{-2} \text{ eV}^{-1}$ to about $6 \times 10^{10} \text{ cm}^{-2} \text{ eV}^{-1}$ as the vicinal angle increased to about 5°.¹⁰ The studies of Yasuda *et al.* were on Si-SiO₂ structures prepared by the same two-step RPAO-RPECVD 300 °C process that has been described above, and is discussed in detail in Ref. 5. Al electrodes were employed and a 400 °C postmetallization anneal (PMA) in a H₂ containing ambient was used. The magnitudes of the incremental increases in D_{it} with increasing vicinal angle indicated that only a relatively small fraction of the dangling bond states at the step edges contributed to increases in D_{it} with increasing step edge density due to increasing vicinal angle.

At the present state of the art, the highest quality SiC crystals for devices are epitaxial layers formed on Si atom terminated 6H SiC vicinal approximately 3.5° in the 1120 direction. Using RPAO-RPECVD, the results of device studies using vicinal 6H *p*-type SiC as reported by Gözlü *et al.*⁷ are markedly different than the results reported for vicinal Si. Metal-oxide-semiconductor (MOS) capacitors were prepared the essentially the same two-step RPAO-RPECVD process as used by Yasuda *et al.*⁵ for Si. However, following a conventional PMA in an H₂ containing ambient, D_{it} values were in excess of $10^{13} \text{ cm}^{-2} \text{ eV}^{-1}$, even when an 1150 °C furnace anneal in Ar was interposed between the oxide film deposition and the metallization steps. However if the high temperature anneal was performed in an H₂ containing ambient then D_{it} values after the conventional 400 °C PMA were reduced significantly into the $10^{11} \text{ cm}^{-2} \text{ eV}^{-1}$ range.⁸ This large difference in defect densities is approximately equal to the number of carbon atom dangling bonds at the step edges suggesting that these dangling bonds were not H-terminated after a conventional 400 °C PMA, but instead required the higher temperature exposure to H for termination. It is important to note that interfaces prepared on the same type of vicinal SiC surfaces by conventional high temperature thermal oxidation processes also required a high temperature anneal in an H₂ containing ambient to yield values of D_{it} in the $10^{11} \text{ cm}^{-2} \text{ eV}^{-1}$ range.¹⁰ Step edge carbon atom dangling bonds on vicinal Si wafers can either be terminated by oxygen atoms that connect into the SiO₂ dielectric, or by hydrogen atoms. The annealing results in Refs. 8 and 10 are consistent with hydrogen atom termination of step edge carbon atom dangling bonds (see Section II for atomic structure at the step edges); i.e., dangling bond elimination

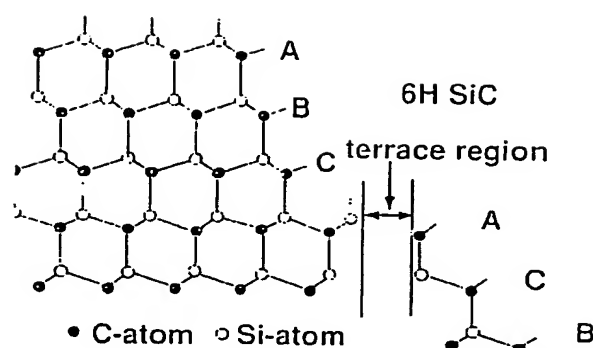


FIG. 1. Schematic representation of surface and step bonding for 6H SiC vicinal wafers. The C atom dangling bonds for the first 6-atom, 3-layer sequence are one per step edge C atom; for the second 6-atom, 3-layer sequence, there are two dangling bonds per step edge C atom. The 6-atom steps are separated by flat terrace regions with Si-atom dangling bonds.

would be accomplished by atomic hydrogen generated during the 1150 °C anneal.

To study interfacial bonding arrangements between SiC and SiO₂, on-line AES has been used to monitor the initial stages of SiC-SiO₂ interface formation. This same approach has been used to study the initial stages of interface formation on Si by both RPAO and rapid thermal oxidation (RTO), and using both O₂ and N₂O oxygen atoms sources gases.⁷ This article extends this approach to SiC and focuses on the initial stages of the RPAO process as applied to both flat or vicinal SiC surfaces using O₂ source gases. Preliminary results are also presented for RPAO using N₂O as the oxygen atom source gas. Section II discusses briefly the local bonding arrangements at the step edges of the vicinal 6H SiC wafers. Section III presents results of AES studies of SiC RPAO, and includes comparisons between the RPAO of SiC and Si. Detailed results are presented for RPAO using O₂, and preliminary results for RPAO using N₂O. Section IV summarizes the major results of this study as they apply to (i) the results of the on-line AES studies, and (ii) the passivation of step edge dangling bonds as revealed by changes reductions in D_{it} levels as determined from electrical measurements.

II. LOCAL BONDING AT STEP EDGES

The dangling bond geometry for Si(111) wafers off cut in the 112 direction has been discussed in Ref. 4 and references therein. The steps are effectively two atom layers high, and the step edge atoms have a single dangling bond. The steps on 6H SiC with Si terminated surfaces are more complex due to the larger unit cell. The repeat pattern of 6H SiC extends over 12 atomic planes of alternating Si and C atoms as shown in Fig. 1. For off cut angles in the 1120 direction, the vicinal Si face surfaces can either include two different 6 atom steps that are separated by Si atom terminated terrace regions, or alternatively consist of six 2 atom layer steps/6H repeat pattern. Figure 1 indicates the bonding arrangements for the two different 6 atoms steps. The first set of steps are in an ABC sequence with one carbon atom dangling bond

per double layer Si-C component, and the second set of steps are an ACB sequence with two carbon atom dangling bonds per double layer Si-C component. The average number of dangling bonds per step in 6H SiC(0001) is 1.5 dangling bonds per step edge atom, whereas in Si(111) off cut in the 112 direction it is only 1 dangling bond per step atom. The spacing between single steps on Si(111) off cut in the 112 direction is ~ 5 nm for a 3.5° off cut angle, so that the ratio of step edge to terrace dangling bonds is approximately 0.06. For a 3.5° off cut angle on SiC, the dangling bond ratio is higher by a factor of 1.5 due to the different step edge terminations of the ABC and ACB sequences. If the 6H SiC surface has two atom steps, as is likely for the wafers used in this study, the dangling bond considerations are the same. Starting with the same ABC sequence as in Fig. 1, the first three 2 atom steps are terminated by C atoms with one dangling, and the second three 2 atom steps by C atoms with two dangling bonds. This means that the number of dangling bonds per step on the average is still 1.5 times greater than for off cut Si wafers.

III. EXPERIMENTAL RESULTS

The samples used in this study were *p*-type 6H SiC purchased from Cree Corporation with Si faces. Similar to polar faces on III-V compounds, the polar faces on SiC are either Si or C faces. Note further that this particular designation is used independent of any surface contamination. One of the wafers was oriented on a principal axis, the (0001) direction, and the other was a vicinal wafer off cut at approximately 3.5° in the 1120 direction. The surface of the on-axis sample was prepared from and bulk ingot, and the surface of the off-axis sample used in these studies was from an epitaxially grown film. The surfaces of the wafers were cleaned following a procedure suggested by Cree Research, Inc.¹¹ The *ex situ* cleaning consisted of (i) sequential rinses in tri-chloroethane (TCE), acetone and methanol, followed by (ii) a conventional two bath RCA clean. The sacrificial oxide formed in the second step of the RCA clean was removed by rinse in dilute HF. Samples were then loaded into a multichamber system, which provides a separate ultrahigh vacuum (UHV) compatible chambers for RPAO and AES. The experimental procedure was to alternate AES measurements with RPAO processing. A similar approach has been applied to RPAO of Si, and through analysis of the AES data, two kinds of information were obtained: (i) the chemical bonding at the Si-SiO₂ interface, and (ii) the oxide thickness as a function of oxidation time.¹²

Figures 2(a) and 2(b), respectively give differential AES spectra for flat and vicinal SiC obtained by RPAO using an O₂ source gas. The experimental processing conditions are:

- (i) a substrate temperature of 300 °C,
- (ii) a process pressure of 300 mTorr,
- (iii) a plasma power to the He/O₂ mixture of 30 W, and
- (iv) flow rates 200 standard cubic centimeters per minute (sccm) of He, and 20 sccm and O₂.

The as-loaded samples show surface contamination by oxy-

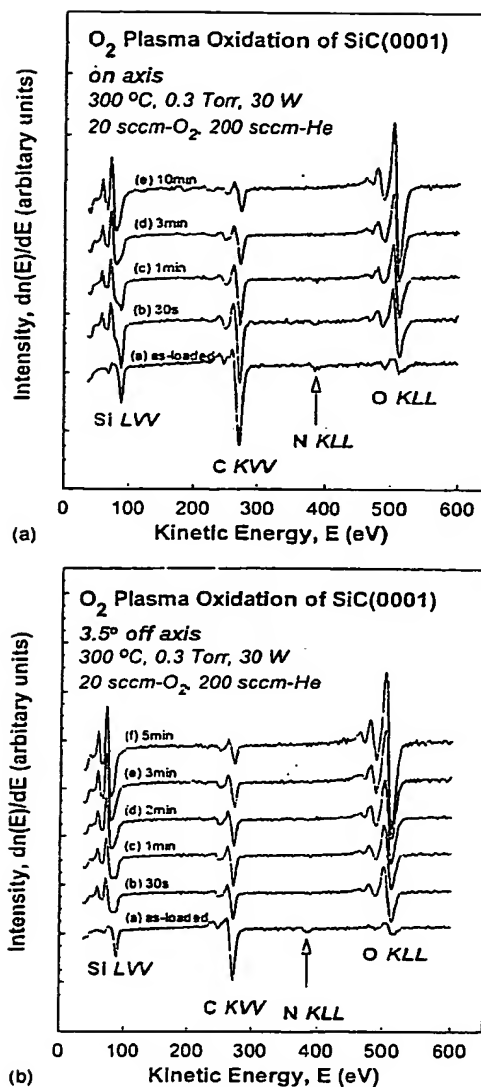


FIG. 2. Derivative mode AES spectra for (a) flat and (b) vicinal SiC obtained by RPAO at 300 °C using O₂ as the oxygen atom source gas.

gen and nitrogen that was not removed by the *ex situ* cleaning process. Since the levels of surface contamination were sub-monolayer, no *in situ* cleaning was attempted. This was in part due to the limited temperature capabilities of the plasma-processing chamber: the substrate heater in this chamber cannot heat a wafer to a temperature greater than about 500 °C. Never-the-less, the nitrogen contamination problem must be overcome before detailed studies of interface bonding using an N₂O source gas can be definitive with respect to any preferential nitrogen atom incorporation at the SiC-SiO₂ interface. It should be further noted that the SiC samples used in this study were *n*-type with a N atom doping level of $\sim 1.4 \times 10^{18} \text{ cm}^{-3}$, so that the N contamination

may have its origin in the doping of the SiC wafers; however, it cannot be attributed simply to the doping because the area density of dopant atoms in a 2 nm thickness (~ 2 electron escape depths) is $\sim 3 \times 10^{11} \text{ cm}^{-2}$, which is considerably less than the minimum AES detection limit of $\sim 10^{13} \text{ cm}^{-2}$. In spite of the sub-monolayer surface N concentration, information relative to oxidation rates could be obtained using the N₂O source gas. In the case of Si, as-loaded samples generally showed small levels of oxygen contamination, but never showed any nitrogen signal, so that more detailed interface bonding studies could be performed with both O₂ and N₂O source gases.¹² Prior to oxidation, the flat and vicinal SiC wafers displayed essentially the same ($\pm 3\%$) Si/C surface ratios so that changes in these ratios could be correlated with the effects of the oxidation processes. As the oxidation time for the SiC wafers is increased, there are four changes evident in the SiC spectra in Figs. 2(a) and 2(b):

- (i) the line shapes and multiplicity of features within the Si_LVV group changed,
- (ii) the C_KVV signal strength decreased,
- (iii) the N_KLL signal strength decreased, and
- (iv) the O_KLL signal strength increased.

These spectral changes are consistent with the growth of an SiO₂ film on the SiC substrate.

Figures 3(a) and 3(b), and 4(a) and 4(b) display, respectively, changes in (a) the Si_LVV and (b) the C_KVV (AES) features as a function of the oxidation time for flat (Fig. 3) and vicinal (Fig. 4) surfaces. Consider first the Si_LVV features in Figs. 3(a) and 4(a). The feature at $\sim 88 \text{ eV}$ is associated with Si-C bonds, in particular with a Si atom that is bonded to four C atoms. As the oxidation proceeds this feature decreases in strength as the Si-O feature at $\sim 76 \text{ eV}$ increases. These changes in relative intensity are due to increase of the oxide thickness with time and are consistent with the relative values of the electron escape depth, $\sim 0.6 \text{ nm}$, and the oxide thickness. There is also a shift of the Si-C feature to lower energy as the oxidation proceeds; this is more easily seen in the spectra for the off-axis sample. Figures 5(a) and 5(b) display the integrated Si_LVV spectra. It is evident from Figs. 3(a) and 5(a) that as the intensity of the Si-C feature decreases, the position of this spectral feature moves to lower energy. In particular in Fig. 3(a), the Si-C feature is evident as a distinct spectral peak at $\sim 88 \text{ eV}$ prior to oxidation, after the oxidation has progressed for 3 min it has shifted to lower energy and appears as shoulder at $\sim 84 \text{ eV}$ on the 76 eV peak. In contrast, the C-Si feature in the C_KVV spectrum in Fig. 4(a) simply decreases in strength as the oxidation process proceeds. The absence of any significant spectral change in this region of the AES spectrum is indicative of the fact that C-O bonds are not formed during the RPAO process. The development of interfacial C-O bonds would produce a satellite peak at lower energy, which would increase in relative strength to the C-Si feature as the oxide growth proceeds and the AES signal becomes more sensitive to the SiC interface than the bulk.

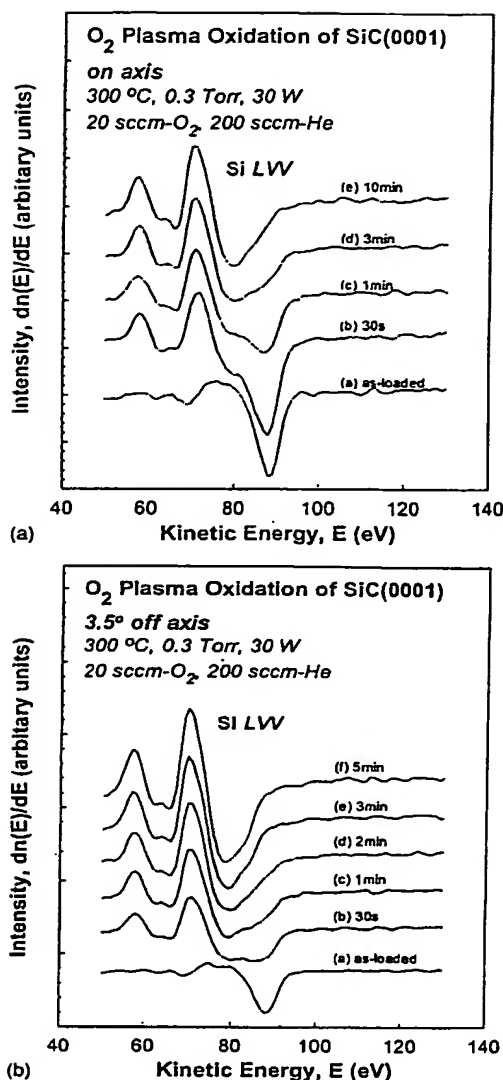


FIG. 3. Changes in the Si_LVV AES features as a function of the oxidation time for (a) flat and (b) vicinal SiC surfaces for O₂ RPAO.

The oxide thickness can be obtained to $\pm 5\%$ from the relative intensity changes in the C_KVV feature using the characteristic escape depth of 0.96 nm for 275 eV electrons. A similar approach has been applied for the determination of the oxide thickness for the RPAO process on Si, and has been validated by a direct measurement of oxide thickness by cross-sectional high resolution transmission electron microscopy.

Figures 6(a) and 6(b) shows log-log plots, respectively of the oxide thickness versus the oxidation time for the RPAO of (a) Si and (b) SiC for the O₂ source gas. In each instance the data can be fit by a power law dependence of the form, $t_{\text{ox}} = At^b$, where t_{ox} is the oxide thickness in nm, t is the oxidation time in minutes, and A and b are fit

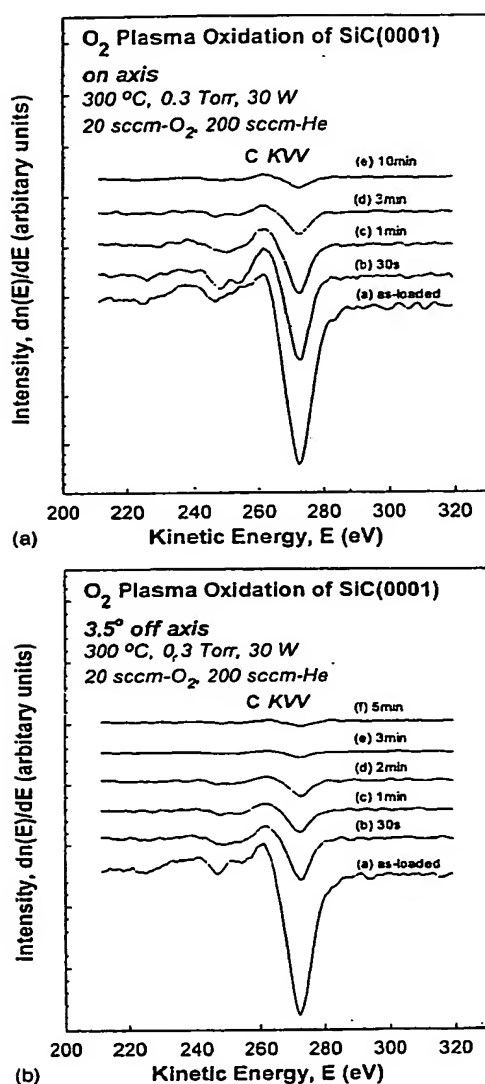


FIG. 4. Changes in the C_{KVV} AES features as a function of the oxidation time for (a) flat and (b) vicinal SiC surfaces for O₂ RPAO.

parameters.^{12,13} The initial oxidation rates are about one and one-half times faster for the vicinal than for the flat wafers, and the initial oxidation rates are faster for Si than for SiC. However, the power law exponents for the SiC oxidations for both flat and vicinal surfaces are greater than the corresponding exponential factor for Si; however, all of these power law exponents are less than 1. The relative differences in the power law factors means that at long times of about 10 min or more the thicknesses of the oxides formed on both Si and SiC are comparable for both the flat and vicinal wafers. Figure 7 illustrates this by showing a comparison of oxide thickness versus oxidation time for flat Si and SiC; a similar situation also prevails for the oxidation of the off-axis wafers.

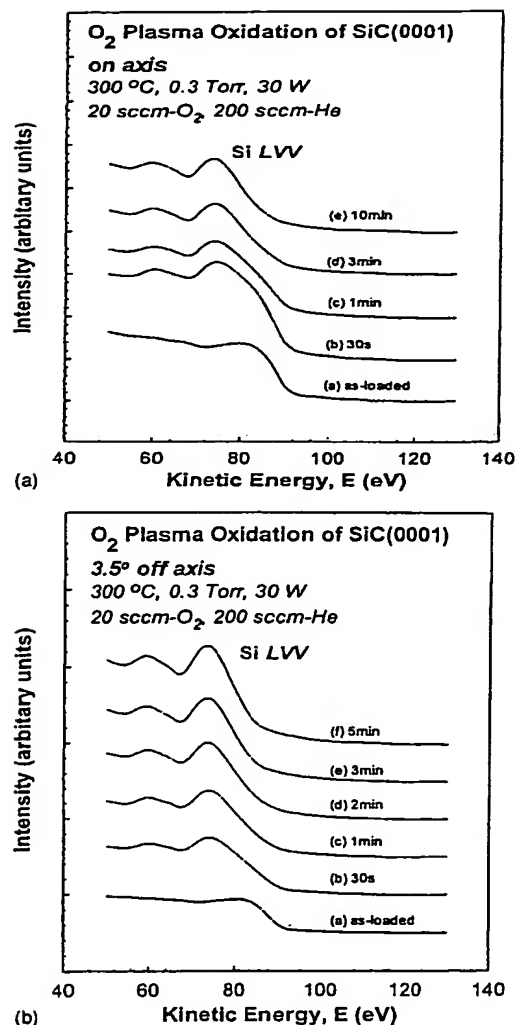


FIG. 5. Integral, $n(E)$, Si_{LVV} AES spectra as a function of the O₂ RPAO oxidation time for (a) flat and (b) vicinal SiC surfaces.

Finally for the RPAO of Si using the same relative flow rates of N₂O and O₂, the oxide growth rate was slower by a factor of 2 using the N₂O source gas.¹² Comparisons of RPAO rates have also been made for SiC for plasma excited O₂ and N₂O source gases. For the same relative flow rates of these two source gases, the situation is reversed with respect to Si, i.e., the oxidation rate of SiC is greater using the N₂O source gas. This increased growth rate using plasma excited species from the N₂O discharge is illustrated in Fig. 8 for the RPAO of flat SiC wafers.

IV. DISCUSSION AND SUMMARY

A. AES results

The analysis of the AES spectra for the flat and vicinal SiC surface RPAO processes using the O₂ source gas indicates:

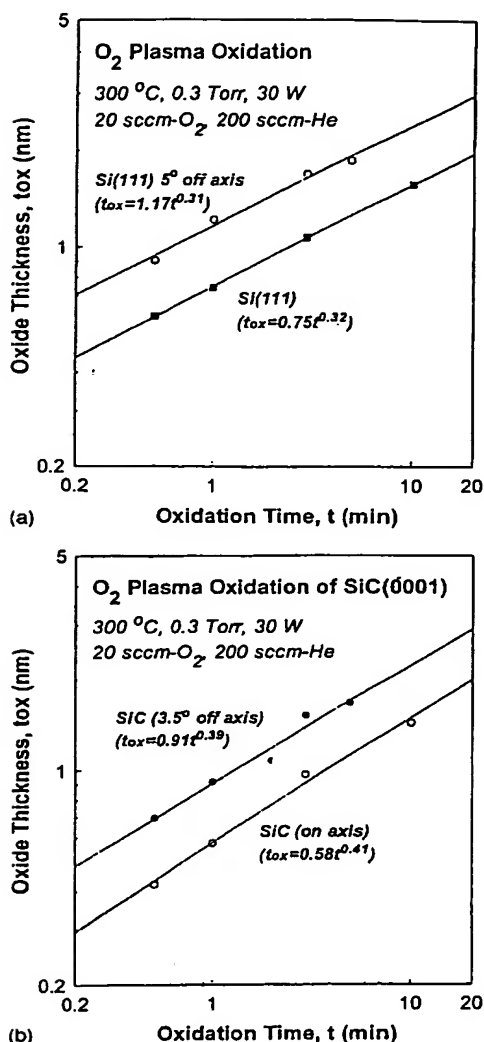


FIG. 6. Log-log plots of the oxide thickness versus the oxidation time for the O₂ RPAO of flat and vicinal (a) Si and (b) SiC. The data are fit to a power law dependence, $t_{ox} = at^b$.

- (i) the solid state oxidation product is SiO₂;
- (ii) there are no interfacial C-O bonds; and
- (iii) oxidation proceeds initially more rapidly on vicinal surfaces than on flat surfaces, paralleling what has been found for Si.

The primary solid state oxidation product for thermal oxidation of SiC is also SiO₂; however, there have been reports of the observation of C-O at or near the SiC-SiO₂ interface.³ This means that there are significant differences in the oxide formation chemistries by low temperature plasma assisted and high temperature thermal oxidation processes. For example, in the plasma assisted processes the oxidation species are typically long-lived molecular metastables such as O₂⁺ or positive molecular ions such as O₂⁺, whereas in the thermal

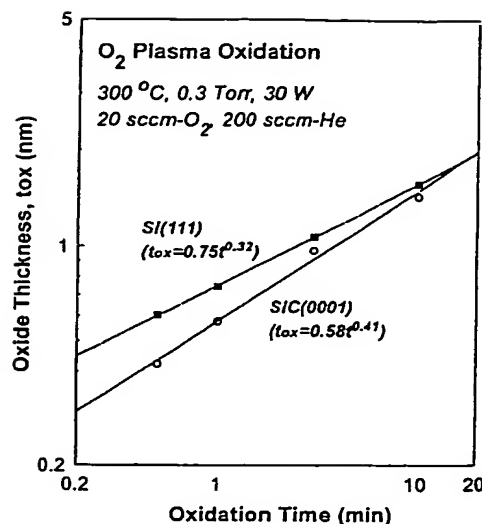


FIG. 7. Log-log plots comparing oxide thickness versus the oxidation time for the O₂ RPAO of flat Si and SiC. The data are fit to a power law dependence, $t_{ox} = at^b$.

oxidation process the oxidation species are typically O atoms. Since the thermal and plasma oxidation processes are qualitatively different with respect to the formation of C-O bonds, then the differences between the two types oxidation processes could be expected to require different post-oxidation and post-deposition procedures for forming low defect density SiC-SiO₂ interfaces. However, this is not the case, as is discussed in Sec. IV B of the article. Before dis-

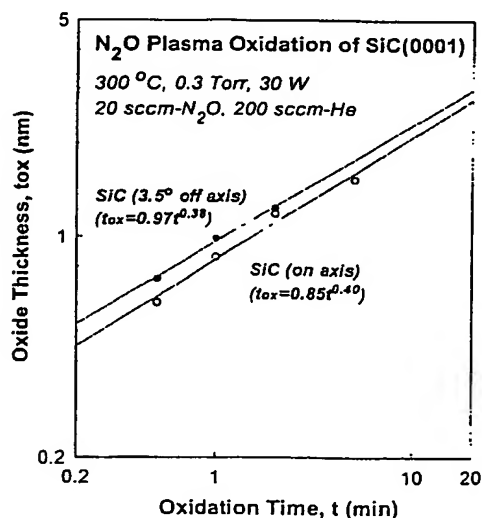


FIG. 8. Log-log plots comparing the oxide thickness versus the oxidation time for the RPAO of flat SiC using O₂ and N₂O as the oxygen atom source cases. The data are fit to a power law dependence, $t_{ox} = at^b$.

cussing this aspect of the experimental results, additional aspects of the power laws fits are discussed below.

The power laws fits to RPAO data show that the oxidation process proceeds very rapidly initially and then slows down considerably with increasing oxidation time. This means chemical reaction rates between excited oxygen species and Si- and Si- and C atom dangling bonds on Si and SiC, respectively, are decreased after Si-O bonds and a superficial layer of SiO₂ are formed at the onset of RPAO.¹⁴

For the case of RPAO of Si the oxidation rate for flat surfaces is faster using O₂ than N₂O for the same relative flow rates of He and O₂ or N₂O. For the RPAO of SiC the situation is reversed for flat surfaces and the oxidation rate is faster using N₂O. Studies are currently underway to address this difference. A model has been proposed for RPAO of Si that explains the differences in the oxidation rates using O₂ or N₂O source gases.¹⁵ This model was developed primarily to explain the retention of nitrogen atoms at the Si-SiO₂ interface during oxide growth using the N₂O source gas. The surface contamination of SiC by nitrogen makes it impossible to determine whether there is nitrogen retention at the SiC-SiO₂ interface during oxide growth in N₂O. This issue is presently under study, and will require the development of procedures for *ex situ* surface preparation that remove residual nitrogen atom contamination from the SiC surface.

B. Electrical properties of SiC-SiO₂ interfaces

This section summarizes results of recent electrical measurements made on MOS capacitors, in particular it compares values of D_{it} as extracted from capacitance-voltage measurements on SiC interfaces prepared on *p*-type substrates. The experimental studies of Stein von Kaminski et al.¹¹ have demonstrated mid-gap D_{it} values in the low $10^{11} \text{ cm}^{-2} \text{ eV}^{-1}$ range for interfaces prepared by high temperature thermal oxidation. These device structures used metal electrodes. The attainment of low defect densities required two annealing steps:

- (i) a post-oxidation an Ar/H₂ mixture at 1150 °C, and
- (ii) a conventional PMA in an H₂ containing ambient at 400 °C after metallization.

When annealing procedures that did not include H₂ in the 1150 °C anneal were applied to the RPAO formed interfaces, the D_{it} values were significantly higher, in the $10^{13} \text{ cm}^{-2} \text{ eV}^{-1}$ range.⁷ However as shown in Ref. 8, these D_{it} values were significantly reduced for the RPAO interfaces following a high temperature (1150 °C) anneal in an Ar/H₂ mixture. It is interesting to note that the difference in D_{it} values between RPAO devices subjected to the Ar and Ar/H₂ anneals is very nearly equal to the density of carbon atom dangling bonds at the step edges. This suggests the possibility that carbon atom dangling bonds are not terminated by during the oxidation or oxide deposition steps, or during the conventional PMA.

Consider first the RPAO interfaces. Since our studies show no C-O bonding in interfacial regions for either the flat or vicinal wafers, it is suggested that the step edge carbon

atom dangling bonds may remain unterminated after the oxidation process. The high defect density after the conventional 400 °C PMA in a hydrogen containing ambient further suggests that the step edge carbon atom dangling bonds are not hydrogen terminated by this process. If this is the case then hydrogen atom production during the 1150 °C anneal in Ar/H₂ is sufficiently high to produce C-H bonding at the step edges. Since thermal oxidation processes show evidence for C-O bonding in interfacial transition regions³ and the RPAO process does not, this suggests that there might be differences related to the way step carbon atom dangling bonds are terminated, either during thermal and plasma oxidations, or in post-oxidation annealing. However, this appears not to be the case, since interfaces produced by high temperature thermal oxidation also require a high temperature anneal in an H₂ containing ambient. This means that even though C-O bonds can be found in silicon oxycarbide transition regions after high temperature thermal oxidation³ they may not be formed in sufficient numbers at carbon atom step edges to neutralize dangling bond defects. Alternatively, the local bonding environment of carbon atoms in interfacial regions and at the Si-C step edges is different and may be a contributing factor to oxygen atom termination.

Finally, it is also interesting to note that fabrication of low D_{it} interfaces on *n*-type SiC by RPAO and thermal oxidation does not require a high temperature anneal in an H₂ containing ambient.⁷ There are two possible explanations for not requiring such an anneal for the RPAO formed interfaces:

- (i) the active interfacial defects are in the bottom half of the SiC band gap and hence are more active in *p*-type material, or
- (ii) the formation of C-O bonds at an SiC interface is Fermi level dependent favoring C-O bond formation in *n*-type material.

The wafers that we studied were nitrogen doped *n*-type wafers, and there was no evidence of interfacial C-O bond formation. However, the concentration of step edge C atom danglings bonds that are available for termination by C-O bonding is below the AES detection limit. 6H SiC flat and vicinal SiC wafers with C faces have been ordered from Cree Research, Inc., upon their receipt, an AES study of the initial stages of PRAO will be initiated. It is clear that these questions identified with respect to electrical results on SiC devices need additional experimental and theoretical studies before they can be satisfactorily resolved. In particular, electron spin resonance experiments that can readily distinguish between Si and C atom dangling bonds may be helpful in resolving the issues discussed in the last two paragraphs.

ACKNOWLEDGMENTS

This research has been supported by the the National Science Foundation, Office of Naval Research, and Air Force Office of Scientific Research (Multi-University Research Initiative).

- ¹L. A. Lipkin and J. W. Palmour, *J. Electron. Mater.* 25, 909 (1996).
- ²T. Ouisse, *Philos. Mag.* B 73, 325 (1996).
- ³B. Hornetz, H.-J. Michel, and J. Halbritter, *J. Mater. Res.* 9, 3088 (1994).
- ⁴J. T. Fitch, E. Kobeda, G. Lucovsky, and E. A. Irene, *J. Vac. Sci. Technol. B* 7, 153 (1989).
- ⁵T. Yasuda, Y. Ma, S. Habermehl, and G. Lucovsky, *Appl. Phys. Lett.* 60, 434 (1992).
- ⁶G. Lucovsky, Yi Ma, S. V. Hattangady, D. R. Lee, Z. Lu, V. Misra, J. J. Wortman, and J. L. Whitten, *Jpn. J. Appl. Phys.* 33, 7061 (1994).
- ⁷G. Lucovsky, A. Banerjee, B. Hinds, B. Claffin, K. Koh, and H. Yang, *J. Vac. Sci. Technol. B*, these proceedings.
- ⁸A. Götz, R. Janssen, E. Stein von Kamiński, and H. Kurz, in *The Physics and Chemistry of SiO₂ and the Si-SiO₂ Interface*, edited by H. Z. Massoud, E. H. Poindexter, and C. R. Helms (Electrochemical Society, Pennington, NJ, 1996), p. 753.
- ⁹C. H. Bjorkman, C. E. Shearon, Jr., Y. Ma, T. Yasuda, G. Lucovsky, U. Emmerichs, C. Meyer, K. Leo, and H. Kurz, *J. Vac. Sci. Technol. B* 11, 964 (1993).
- ¹⁰T. Yasuda, D. R. Lee, C. H. Bjorkman, Y. Ma, U. Emmerichs, C. Meyer, K. Leo, and H. Kurz, *Mater. Res. Soc. Symp. Proc.* 315, 375 (1993).
- ¹¹E. Stein von Kamiński *et al.*, *Microelectron. Eng.* 28, 201 (1995).
- ¹²G. Lucovsky, H. Niimi, K. Koh, D. R. Lee, and Z. Jing, in *Ref. 8*, p. 441.
- ¹³D. R. Wolters and A. T. A. Zegers-van Duynhoven, *J. Appl. Phys.* 65, 5126 (1989).
- ¹⁴P. Thanikasalam, T. K. Whidden, and D. K. Ferry, *J. Vac. Sci. Technol. B* 14, 2840 (1996).
- ¹⁵K. Koh, H. Niimi, and G. Lucovsky, *Mater. Res. Soc. Symp. Proc.* (in press).